27
11-15-82
88
I-6404

1

Dr. 978

SERI/TP-252-1415
UC Category: 64

SERI/TP--252-1415

DE83 002462

A Study of Falling-Jet Flash Evaporators

F. Kreith
D. A. Olson
D. Bharathan
H. J. Green

MASTER

November 1982

Prepared Under Task No. 1111.00
WPA No. 09-244

Solar Energy Research Institute
A Division of Midwest Research Institute

1617 Cole Boulevard
Golden, Colorado 80401

Prepared for the
U.S. Department of Energy
Contract No. EG-77-C-01-4042

DISCLAIMER

ABSTRACT

Experimental results of flash evaporation from sheets of water, 3.2 mm and 6.3 mm thick and 27.9 cm wide, falling freely in the presence of their own vapor, are reported. With no flashing the jets fall in coherent sheets, but with flashing the jets were observed to spread and break up into droplets. Flashing was characterized by an effectiveness parameter, which was found to increase with increasing water temperature and jet length. Variations in water flow rate and heat flux did not influence the effectiveness appreciably.

1. INTRODUCTION

Direct-contact heat transfer is an area of current research interest for several reasons. First of all, there are many applications in which the heat exchange surfaces constitute a major portion of the expense of the total system and are subject to problems such as corrosion, fouling, and maintenance. Furthermore, whenever a solid surface separates two fluids between which heat is exchanged, a substantial temperature difference is required to transfer the heat and this temperature difference results in a loss of overall system thermal efficiency. Examples of such situations can be found in geothermal systems, in ocean thermal energy conversion systems, in bottoming cycles which are being considered for power plants situated near low-temperature sinks, in solar ponds, and in total energy systems in which the available temperature difference is small. In other words, as we move into an era when high quality energy is becoming more expensive and less available, methodologies which can enhance the heat transfer efficiency and reduce the deterioration in the energy quality available for doing productive work becomes increasingly important. The work reported in this paper deals with one phase of direct contact heat transfer problems, namely the heat and mass transfer between two streams of the same fluid in which a liquid jet is undergoing a phase change by evaporation in direct contact with its own vapor.

eb

2. EXPERIMENTAL APPARATUS

We investigated evaporation from falling jets of water, ranging in water inlet temperatures from 15^{o} to $40^{o}C$. The jets were either 3.2 or 6.3 mm wide, with lengths between 0.28 and 0.74 m. For either jet, the specific flow rate Γ of water varied from 0.01 to 0.06 m^2/s. The experimental apparatus, shown in Figure 1, consists of a test cell which houses the falling jets, and warm and cold water loops which supply heat to and remove heat from the jets [1,2]. The warm water loop consists of a pump, a heat exchanger with a bypass, a static mixer, a turbine flow meter, and the falling jet in an evaporator module. The valve downstream of the turbine flow meter regulates the flow rate to the test cell, from 3 kg/s to 15 kg/s. The heat exchanger is supplied with hot water from a boiler with a heating capacity between 50 kW and 300 kW. The cold water loop is similar to the warm loop, except that the cold water is piped directly to a chiller with a cooling capacity that matches the boiler heating capacity. Falling jets of cold water condense the vapor generated during evaporation. An interconnecting pipe between the loops replenishes the fluid lost during evaporation to the warm loop.

The test cell is a horizontal cylinder, 1.5 m in diameter and 1.8 m long. Reservoirs underneath the evaporator and condenser sections of the test cell allow separate collection of the warm and cold water. Glass ports on the top and side provide for lighting, viewing, and photography. The cell can be evacuated to 700 Pa. Air leakage rates in the experimental apparatus are less than 1 mg/s so that flashing conditions at all evaporator water temperatures can be achieved. The evaporator module is a rectangular box 0.50 m wide, 0.31 m deep, and 0.74 m high (see Figure 2). A 7.3-cm O.D. pipe with either a 3.2 mm wide or a 6.3 mm wide and 27.9 cm long slot at the bottom along the entire pipe length was used to produce a vertically falling sheet of water. The distance between the sheet of water and the right-side wall is 19 cm. The front panel of the module is made of plexiglas to permit viewing and photographing. The floor of the module was made of two 6.4 mm plexiglas sheets, each with five 2.5 cm wide slots for water drainage. The top sheet could be moved over the bottom sheet by a motor drive to restrict the water flow, thereby varying the height of a water pool above the sliding sheets and thus effectively controlling the evaporator jet length. The steam

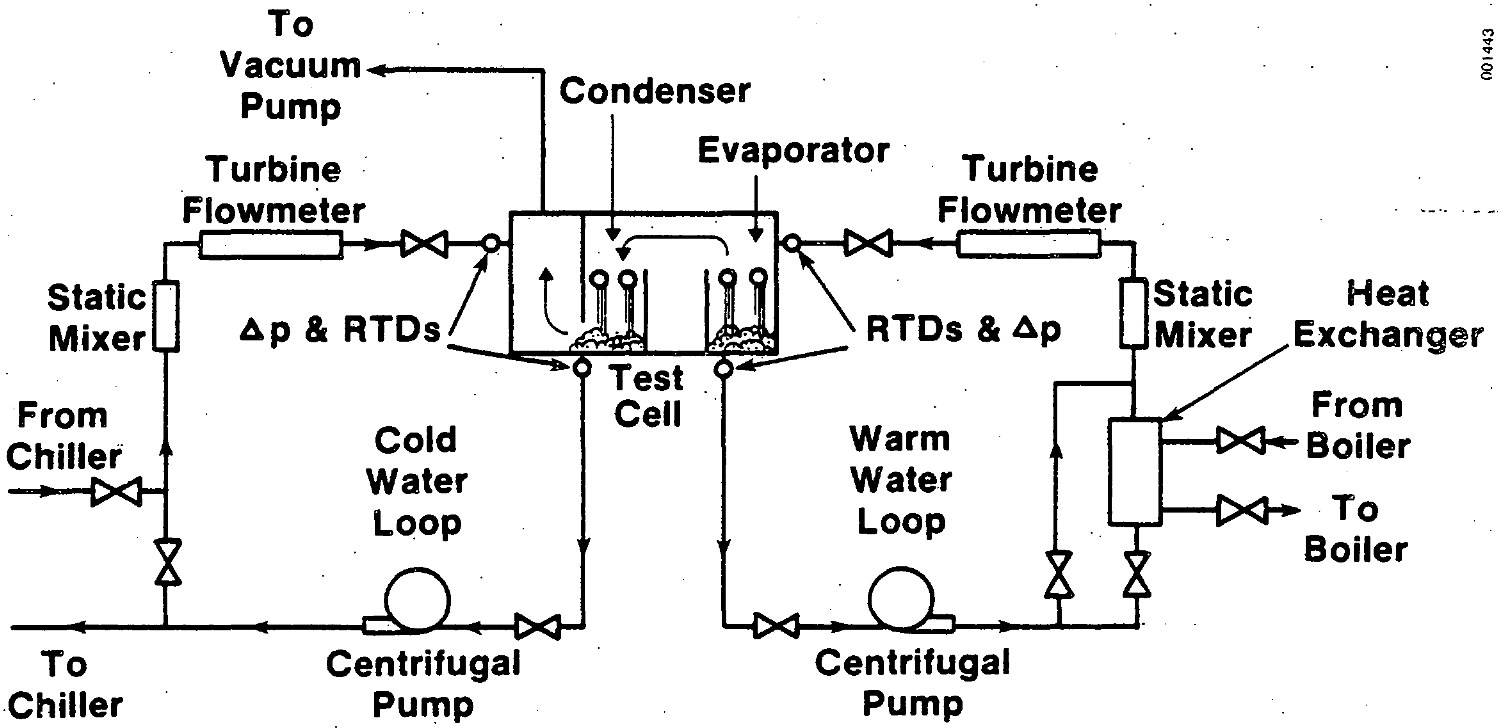

Figure 1. Schematic Diagram of the Experimental Apparatus.

generated in the evaporator flows vertically upward, countercurrent to the liquid flow, past the water inlet pipe. The vapor is diverted horizontally to flow towards two condenser modules with geometry similar to the evaporator module, each with 4 falling jets of water. Due to the structure of the test loop, which was designed primarily for open cycle ocean thermal energy conversion applications, testing of fluids other than water is not possible with the present apparatus.

3. INSTRUMENTATION AND ACCURACIES

The warm and cold water flow rates are measured using two turbine flow meters, each connected to a flow rate indicator and a frequency counter. The pressure loss in each liquid stream across the test cell is measured using a variable reluctance pressure transducer. Temperature in the liquid streams is measured with platinum resistance temperature detectors (RTD). Wet-bulb vapor temperatures are measured by three RTDs above the evaporator (see Figure 2) and condenser modules, at

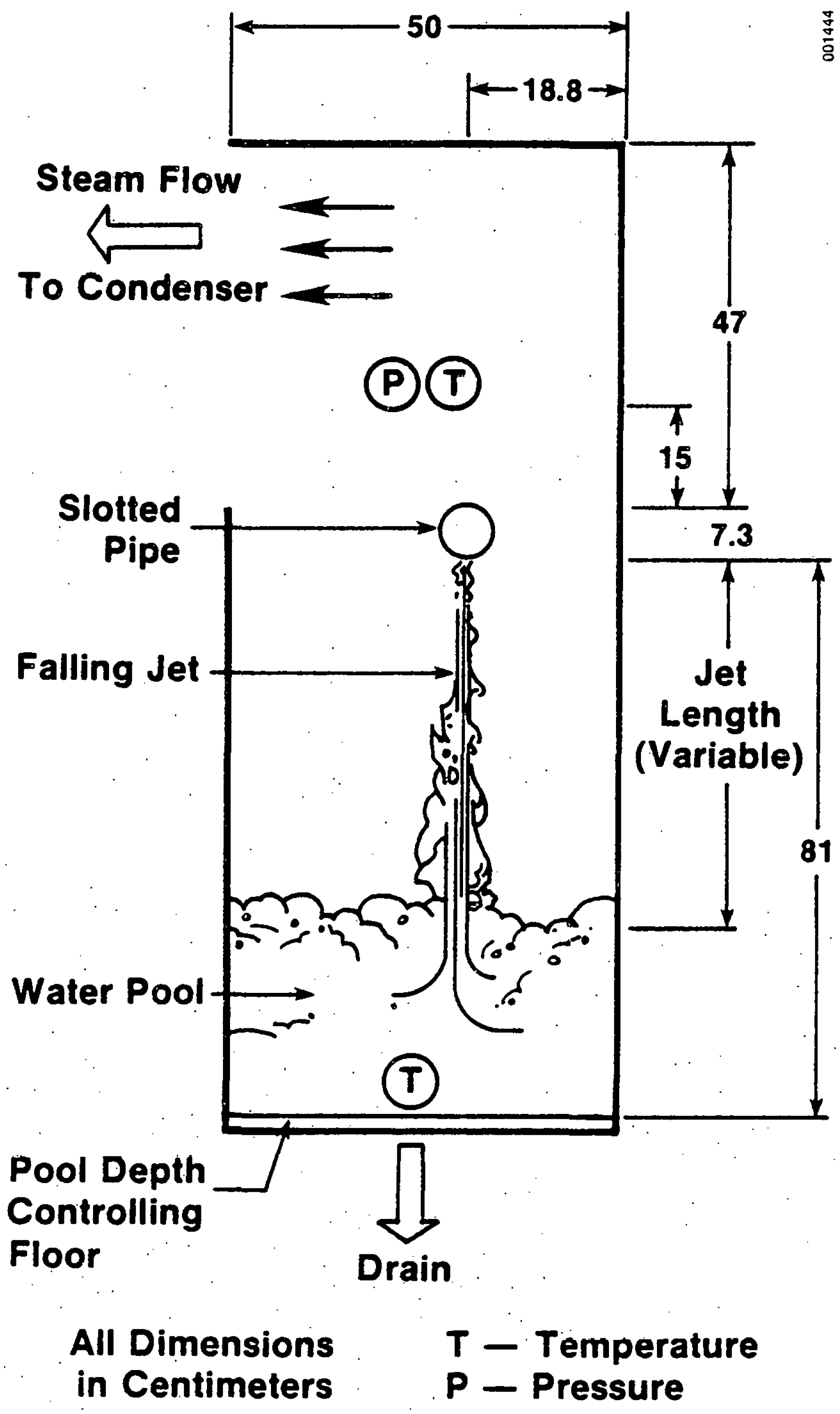

Figure 2. Cross-Sectional Front View of the Evaporator Module (All Dimensions in Centimeters)

three locations within the test cell. The vapor RTDs are blanketed with cotton wicks wetted from a water reservoir. Static pressure in the steam flow path is measured at three locations next to the temperature sensors using wall pressure taps and three differential pressure transducers with the reference sides evacuated. In the evaporator module, the steam temperature sensor and the pressure port are located outside of possible wake regions downstream of the slotted pipe. A meter stick mounted on the front panel permits visual monitoring of the jet length. RTD resistance and pressure transducer voltages are scanned through a data acquisition control unit and digitized with a digital voltmeter. All data are collected through a desk-top computer and stored on magnetic tape.

Uncertainties in temperature measurements arise from calibration errors in the RTD probe, self heating, stem conduction, background radiation, and random errors in reading. The uncertainties in the liquid temperature measurements are estimated to be $\pm 0.015^{o}C$ and in the vapor stream $\pm 0.02^{o}C$. Uncertainties in flow rate measurements arising from calibration errors in the flow meter and random errors in reading are estimated as ± 0.14 kg/s. Estimates of similar uncertainties in the liquid pressure loss are ± 1.5 kPa; and in the vapor static pressures are the larger of ± 20 Pa or 0.25%. Uncertainties in the jet length, which represent the largest source of experimental error, are estimated as ± 3 cm.

Based on random error propagation analysis, for a nominal experimental condition (150 kW heat flux; 7 kg/s liquid flow rate; 0.74 m jet length; and $30^{o}C$ inlet temperature), the uncertainty in the reported evaporator effectiveness, ε (see Equation 3), is estimated to be ± 0.003. For a low heat flux, the uncertainty in ε is ± 0.006.

Systematic errors in the effectiveness may arise from a high reading of the vapor temperature due to warmer entrained liquid splashing on the probe and from drifts in temperatures. Simultaneous measurements of vapor temperature and pressure indicate errors in measured vapor temperature due to liquid entrainment may be $+0.02^{o}C$, corresponding to an error in ε of $+0.008$. With the maximum anticipated temperature drift, systematic error in the effectiveness is estimated as ± 0.004, with the sign depending upon the direction of drift.

4. EXPERIMENTAL PROCEDURE

For each jet width, four independent parameters can be varied during an experiment: water flow rate, water inlet temperature, the jet length, and the rate of heat transfer. In a typical run, the warm and cold water pumps are started and the appropriate flow rates are established. Adjusting height-control floor of the pool sets the evaporator jet length. The boiler and chiller loads determine the heat rate. Mismatching the heat fluxes drifts the system temperatures up or down to achieve the equilibrium evaporator inlet temperature. When steady state is established (temperature drifts of less than $2^{o}C$/hour) in both loops, the computer records the data for one experimental point. Individual measurements are averaged ten times for each data point.

5. DATA ANALYSES

Consider a steady-state flashing process where water at an inlet mass flow rate of m_i and temperature T_i produces vapor at a rate of m_v at a temperature T_{sat} in an evaporator and emerges at a temperature T_o. If Δp is the pressure loss in the liquid stream between where T_i is measured and evaporator inlet, then, to account for mechanical energy losses, an effective corrected inlet temperature may be defined as

$$T_c = T_i + \frac{v\,\Delta P}{c_p} \tag{1}$$

Similarly if the vapor, as it emerges from the evaporator, has gained significant kinetic energy and undergone a loss in pressure (i.e., expanded flow work), the effective vapor temperature as it emerges from the liquid within the evaporator would be higher than T_{sat}. Under conditions where the changes in vapor temperature may be negligible and liquid entrainment in the vapor stream is minimal, the vapor production rate can be related to the inlet and outlet conditions of the liquid stream from an energy balance on the evaporator in the form

$$m_v = m_i \frac{e_c - e_o}{e_{sat} - e_o} \tag{2}$$

where e_c is the enthalpy of water at the corrected temperature T_c, e_o is the enthalpy at T_o, and e_{sat} is the enthalpy of vapor at T_{sat}.

We characterize the performance of the evaporator by a heat exchanger effectiveness ε defined as

$$\varepsilon = \frac{T_c - T_o}{T_c - T_{sat}} \quad . \tag{3}$$

If no vapor losses occur between the bottom and top of the evaporator and the vapor temperature is constant, ε is the ratio of the actual heat transferred to the maximum possible if the liquid reached equilibrium with the vapor. Since, due to the jet break-up (discussed below), the interfacial area for heat transfer remains uncertain, we do not attempt to define a heat transfer coefficient.

The results of the experiments are presented as plots of the evaporator effectiveness ε as a function of the experimental variables, namely, water inlet temperature T_c (°C), the water specific flow rate Γ (m^2/s), and the jet length to thickness ratio L/t. Attempts to choose suitable nondimensional variables to represent the effects of temperature and water flow rate have thus far been unsuccessful, because of difficulties in selecting appropriate normalizing temperature and a length scale to characterize the heat-transfer process. The extent of the data is also limited to the parameter ranges particularly applicable to ocean energy systems.

6. DISCUSSION OF RESULTS

A comparison of the physical structure of the 3.2-mm water jet with and without flashing is illustrated by two photographs in Figure 3. The water specific flow rate Γ is 0.026 m^2/s, and the heat flux for the flashing condition is 530 kW per square meter of planar projected jet area. With no heat transfer (Figure 3a), the jet falls in a coherent sheet. Distentions and indentations of the liquid/vapor interface are seen with droplets breaking off, but the overall appearance is of a continuous structure. With heat transfer (Figure 3b), the jet spreads and bursts into many fragments and droplets. The break-up occurs within a few centimeters downstream of the slot; the location of the initial break-up does not appear to vary with any of the experimental parameters. We

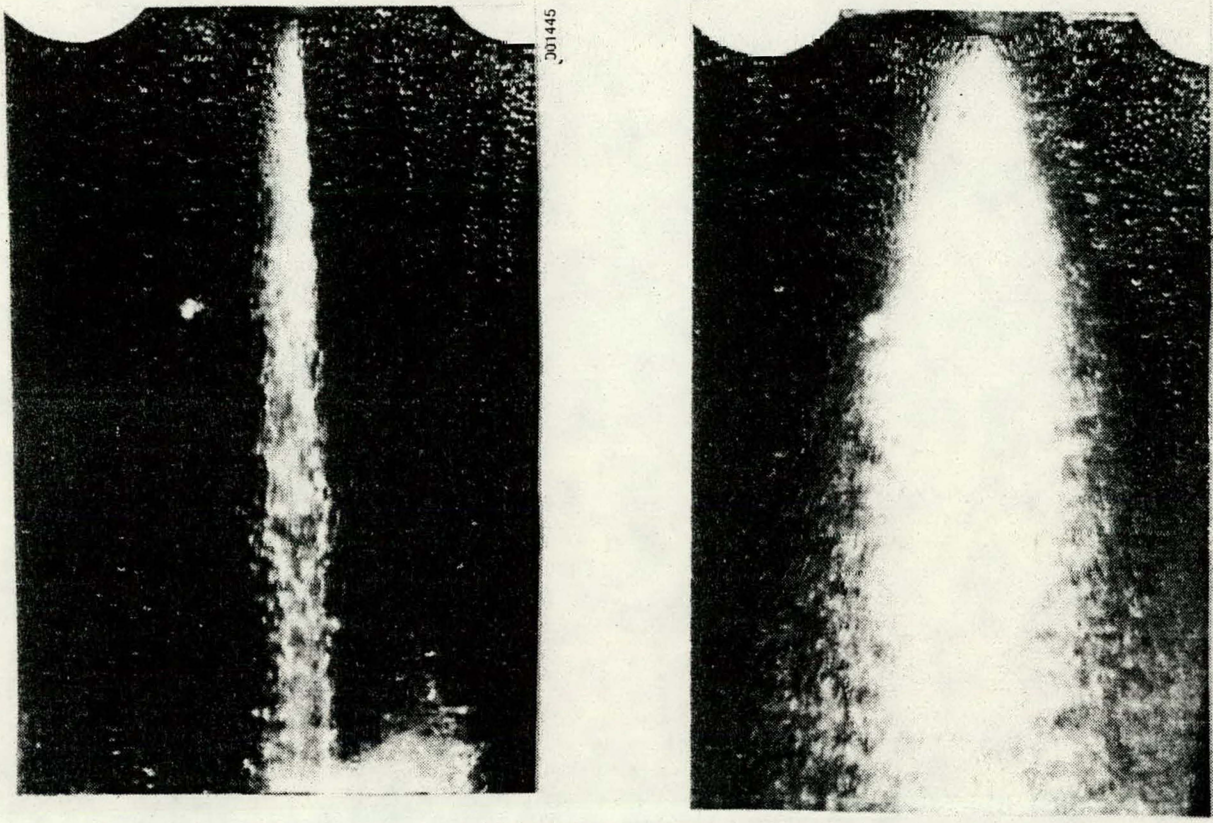

Figure 3. Comparison of the Physical Jet Structure Without (a) and With (b) Flashing.

believe the break-up is due to growth of vapor bubbles from nucleation sites within the jet. Although no measurements of the drop sizes were made, the drops appear to range from fractions of a millimeter to a few millimeters in diameter.

Similar break-up of flashing circular water jets has been observed by others [3,4]. Both these investigators also observed jets without break-up at low heat transfer rates. In Miyatake's experiments [4], for 3-mm and 5-mm diameter jets, the jets remained coherent at temperature differences between the incoming liquid and the vapor up to $4^{o}C$. However, in our tests, the water sheets were observed to shatter even for the lowest liquid/vapor temperature difference of $3.1^{o}C$. We believe these differences in breakup between circular and planar jets result from the differences in geometries of the entrances and the jets themselves.

7. RESULTS

The experimental results are displayed in Figures 4, 5, and 6. Experimental errors are approximately the size of the data symbols. The effect of jet length to thickness ratio, L/t, on the evaporator effectiveness ε for a 6.3-mm jet and a 3.2-mm jet is shown in Figure 4. The specific flow rate is approximately 0.025 m^2/s for both jets, while T_c is 23°C for the 6.3-mm jet and 31°C for the 3.2-mm jet. The effectiveness increases monotomically with increasing L/t for both jets, from 0.7 at L/t = 50 to 0.85 at L/t = 220. Both the 3.2-mm jet and the 6.3-mm jet data appear to merge together, indicating that the length over which the jet breaks up may be related linearly to the jet thickness.

Figure 5 shows the effect of varying the water inlet temperature T_c. In this figure, for the 3.2-mm jet, Γ = 0.025 m^2/s and L/t = 230, and for the 6.3-mm jet, Γ = 0.03 m^2/s and L/t = 120. For either jet, increases in T_c result in approximately linear increases in the effectiveness. At 15°C, ε is nearly 0.7, and at 40°C, ε is 0.85. The increase in effectiveness with temperature could be due to larger saturation pressure variation with temperature at higher temperatures and decreased liquid viscosity. At higher temperatures, a given liquid/vapor temperature difference results in larger driving pressure differences for vapor bubble growth and jet break-up. Effects of any vapor flow losses are also diminished. It is also possible that reduced liquid viscosity at higher temperatures increases jet turbulence and reduces turbulence decay.

Figure 6 shows the effect of varying the specific flow rate on the evaporator effectiveness. For the 3.2-mm jet, T_c = 28.5 to 30.3°C and L/t = 230. For the 6.3-mm jet, T_c = 22°C and L/t = 116. (L/t = 108, 100, and 88 respectively for the three largest Γ values, with increasing Γ, due to apparatus limitations.) The effectiveness remains roughly constant at nearly 0.85 for the 3.2-mm jet. ε decreases somewhat for the 6.3-mm jet at high values of Γ; this decrease is partly due to decreases in L/t as noted above.

Experiments were also conducted with heat rates varying from 250 to 720 kW per square meter of jet area at nearly constant T_c, Γ, and L/t. The jets appeared to undergo nearly the same extent of break-up at all heat rates, and generally minimal change in the evaporator effectiveness was observed.

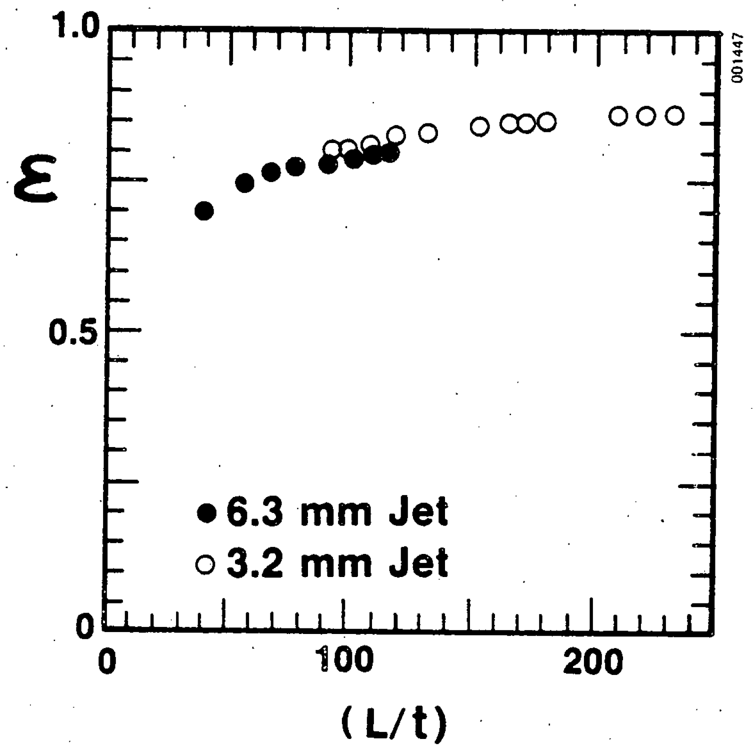

Figure 4. Effect of Jet Length on Evaporator Effectiveness

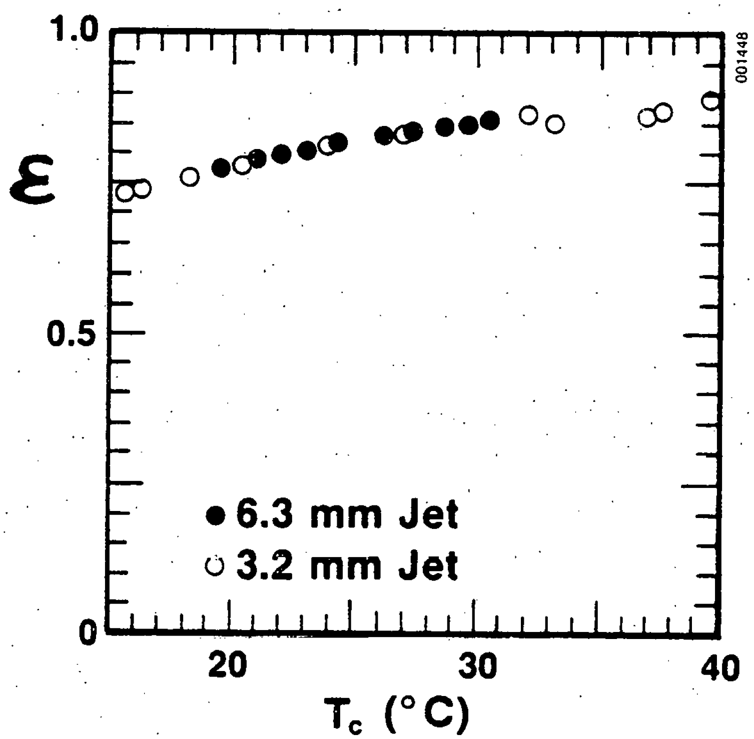

Figure 5. Effect of Water Inlet Temperature on Evaporator Effectiveness

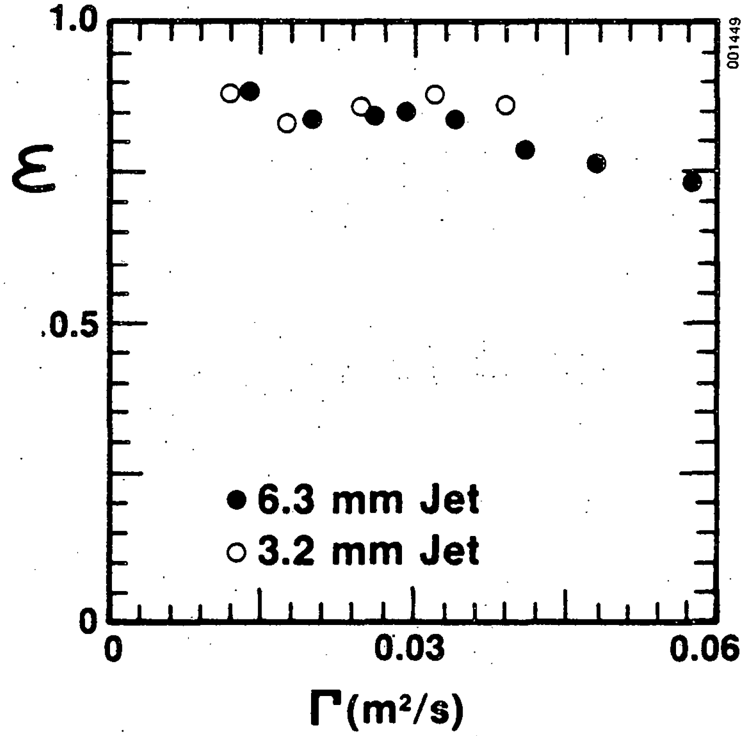

Figure 6. Effect of Water Specific Flow Rate on Evaporator Effectiveness

Some difficulties in selecting the proper non-dimensional variables for data correlations are illustrated by plotting the effectiveness versus a liquid Reynolds number Re for the 3.2-mm jet in Figure 7. For this plot, Re is defined as

$$Re = \frac{\rho_\ell V t}{\mu_\ell} \tag{4}$$

where ρ_ℓ is the liquid density and μ_ℓ is the liquid viscosity, both at the inlet temperature T_c. This figure, a composite of Figure 5 and 6, illustrates how changes in T_c and Γ affect ε. When Re is increased by increasing Γ at constant T_c, the effectiveness remains nearly constant. However, when Re is increased by increasing T_c at constant Γ, ε increases with Re. Thus, the present form of Re based on jet thickness is not appropriate or sufficient to correlate evaporator effectiveness. Similarly, attempts to relate ε to a Jacob number, defined as

$$Ja = \frac{\rho_\ell c_p (T_c - T_{sat})}{\rho_v h_{fg}} \tag{5}$$

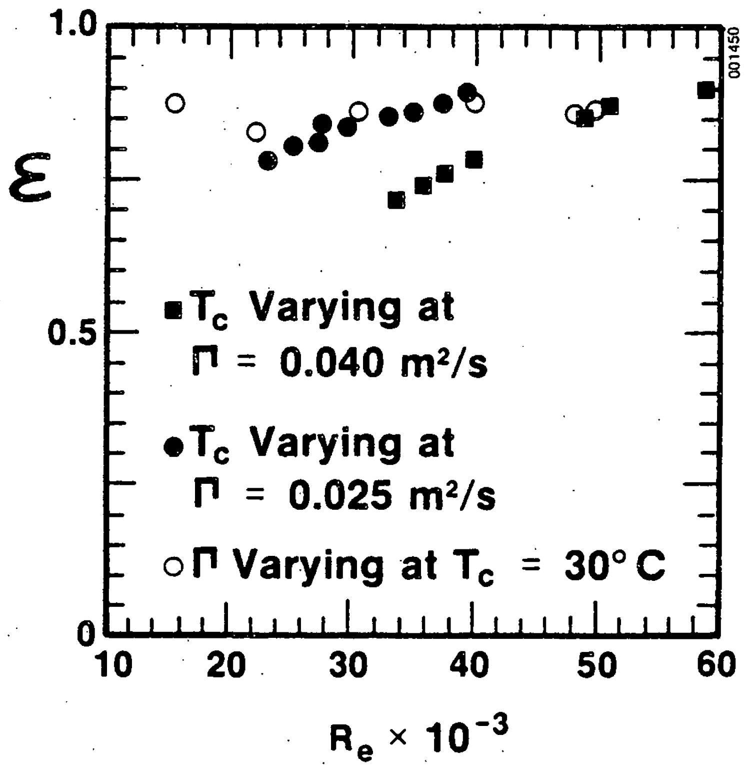

Figure 7. A Plot of Effectiveness, ε versus Liquid Reynolds Number, Re for the 3.2 mm Jet, Showing Different Trends when varying Γ and when varying T_c to change Re.

where unsuccessful. Different trends in ε versus Ja were observed when Ja was changed by varying ρ_v (through T_c) and by varying $T_c - T_{sat}$ (through Γ and heat flux).

8. CONCLUDING REMARKS

This paper presents initial data on flash evaporation from planar sheets of water falling in the presence of their own vapor. For the two jet thicknesses investigated, the evaporator effectiveness increases with increasing liquid temperature and jet length, but remains almost constant or decreases slightly with increasing liquid flow rate.

NOMENCLATURE

c_p	specific heat of water (kJ/kg K)
e	enthalpy (kJ/kg)
h_{fg}	latent heat of vaporization (kJ/kg)
Ja	jacob number
L	jet length (m)
m	mass flow rate (kg/s)
Re	liquid Reynolds number
T	temperature (°C)
t	jet thickness (mm)
V	liquid inlet velocity (m/s)
v	liquid specific volume (m^3/kg)
Γ	specific flow rate (m^2/s)
Δp	pressure loss (Pa)
μ_ℓ	liquid viscosity (kg/m s)
ε	evaporator effectiveness
ρ_ℓ, ρ_v	liquid and vapor densities (kg/m^3)

SUBSCRIPTS

c	corrected inlet
i	inlet
ℓ	liquid
o	outlet
sat	saturated vapor
v	vapor

REFERENCES

1. Kreith, F., An Overview of SERI Solar Thermal Research Facilities, Heat Transfer Engineering, vol. 2 (Nos. 3-4), pp. 16-19, January-June 1981.

2. Green, H. J., Olson, D. A., Bharathan, D., and Johnson, D. H., Measured Performance of Falling-Jet Flash Evaporators, SERI/TP-631-1270, June 1981.

3. Balitskiy, S. A., and Shurchkova, Yu. A., Flashing of a Superheated Liquid Under Vacuum, Heat Transfer - Soviet Research, vol. 1, (No. 3), pp. 106-109, May 1969.

4. Miyatake, O., Tomimura, T., Ide, Y., and Fujii, T., An Experimental Study of Spray Flash Evaporation, Desalination, vol. 36, pp. 113-128, 1981.